Biochemical and Biophysical Research Communications 516 (2019) 1229–1233

Contents lists available at ScienceDirect

Biochemical and Biophysical Research Communications

journal homepage: www.elsevier.com/locate/ybbrc

Postnatal Runx2 deletion leads to low bone mass and adipocyte accumulation in mice bone tissues

Ikue Tosa [a, b], Daisuke Yamada [a], Misa Yasumatsu [a], Eiichi Hinoi [c], Mitsuaki Ono [d], Toshitaka Oohashi [d], Takuo Kuboki [b], Takeshi Takarada [a, *]

[a] Department of Regenerative Science, Okayama University Graduate School of Medicine, Dentistry and Pharmaceutical Sciences, Okayama, 700-8558, Japan
[b] Department of Oral Rehabilitation and Regenerative Medicine, Okayama University Graduate School of Medicine, Dentistry and Pharmaceutical Sciences, Okayama, 700-8558, Japan
[c] Laboratory of Molecular Pharmacology, Division of Pharmaceutical Sciences, Kanazawa University Graduate School, Kanazawa, Ishikawa, 920-1192, Japan
[d] Department of Molecular Biology and Biochemistry, Okayama University Graduate School of Medicine, Dentistry and Pharmaceutical Sciences, Okayama, 700-8558, Japan

ARTICLE INFO

Article history:
Received 26 June 2019
Accepted 5 July 2019
Available online 9 July 2019

Keywords:
Runx2
Conditional knockout
Aging
Osteoporosis
Bone marrow adiposity

ABSTRACT

Global gene deletion studies have established that Runt-related transcription factor-2 (Runx2) is essential during skeletogenesis for osteoblastic differentiation in both intramembranous and endochondral ossification processes. However, the postnatal significance of Runx2 *in vivo* is poorly understood because a global Runx2 deletion causes perinatal lethality. In this study, we generated tamoxifen-induced Runx2 global deficient mice by crossing $Runx2^{flox}$ mice with $ROSA26\text{-}CreER^{T2}$ mice ($Rosa26\text{-}CreER^{T2}$; $Runx2^{flox/flox}$). Four-week-old mice were intraperitoneally treated with tamoxifen for five consecutive days, sacrificed, and analyzed six weeks after tamoxifen administration. Deletion of Runx2 led to low bone mass, which is associated with decreased bone formation and bone resorption as well as excessive bone marrow adiposity. Collectively, postnatal Runx2 absolutely plays an important role in maintaining the homeostasis of bone tissues not only in bone mass, but also in the bone marrow environment.

1. Introduction

Bone formation and resorption are tightly regulated by bone-forming osteoblasts and bone-resorbing osteoclasts, respectively [1,2]. The osteoblast lineage is derived from primitive multipotent mesenchymal stem cells, whereas the osteoclasts are multinucleated cells derived from the fusion of mononuclear hematopoietic precursors. Osteoporosis is a common skeletal disease, especially in the aged human population, and is attributed to diminished osteoblast production and function. Osteoblast reduction and increased adipocyte content in the bone marrow (BM) upon aging are involved not only in decreased bone formation, but also in aging-associated hematopoietic changes, including preferential differentiation, into myeloid accompanied with the loss of B cell lineage [3–6]. Thus, investigations on osteoblast maintenance in BM have a direct medical significance.

The runt-related transcription factor 2 (Runx2) is a member of the Runt family of transcription factors, which play a critical role in cellular differentiation processes of osteoblasts in mice and in humans [7–9]. Experiments using global Runx2 deletion ($Runx2^{-/-}$) mice [10,11] showed that Runx2 is necessary to induce osteoblast differentiation. Runx2 is tightly regulated by several factors, including MAF [12], TAZ [13], pRb [14] and Twist [15]. It regulates multiple osteoblastic genes that determine osteoblastic phenotypes. There is accumulating evidence showing Runx2's importance during skeletogenesis in developmental stages; however, its role in postnatal stages, such as during bone remodeling, remains

Abbreviations: BCA, bicinchoninic acid; BFR/BS, Bone formation rate/bone surface; BM, bone marrow; BV/TV, bone volume/tissue volume; Ct.Wi, cortical width; dnRunx2, dominant negative Runx2; N.Ob/B.Pm, number of osteoblasts per bone perimeter; N.Oc/B.Pm, number of osteoclasts per bone perimeter; Ob.S/BS, osteoblast surface per bone surface; Oc.S/BS, osteoclast surface per bone surface; OPN, Osteopontin; PFA, paraformaldehyde; PLIN, perilipin; PVDF, polyvinylidene difluoride; qPCR, quantitative RT-PCR; Runx2, Runt-related transcription factor-2; TRAP, Tartrate-resistant acid phosphatase.

* Corresponding author. 2-5-1 Shikata-cho, Kita-ku, Okayama, 700-8558, Japan.
E-mail address: takarada@okayama-u.ac.jp (T. Takarada).

https://doi.org/10.1016/j.bbrc.2019.07.014
0006-291X/

poorly understood since global Runx2 deletion leads to perinatal lethality [10,11]. To improve our understanding of Runx2 functions *in vivo*, we previously generated conditional knockout mice carrying a conditional Runx2 allele within exon 4, which encodes the Runt domain, flanked by loxP sites [16]. This mouse model allowed Runx2 characterization in specific cells [17] as well as its postnatal role *in vivo* using a tamoxifen-inducible CreER^{T2} system.

Here, we generated mice that allowed an induced Runx2 gene deletion in adult mice by crossing *Runx2^{flox}* mice with *ROSA26-CreER^{T2}* mice, wherein the recombination of loxP-floxed allele occurred throughout the body upon tamoxifen administration. We observed that postnatal Runx2 deletion led to low-turnover osteoporosis and adipocytes accumulation in the BM. Thus, our data demonstrated that Runx2 deletion in adult mice led to aging-associated phenotypes in BM.

2. Materials and methods

2.1. Experimental animals

Rosa26-CreER^{T2} mice were kindly provided by Dr. Tyler Jacks (Massachusetts Institute of Technology) [18]. Runx2 conditional knockout mice, floxed exon 4 of the *Runx2* gene (*Runx2$^{flox/+}$*) mice [16], were bred in the in-house animal facility at Department of Animal Resources, Advanced Science Research Center, Okayama University. All animal experiments were approved by the Committee on Animal Experimentation of Okayama University and performed in compliance with University Guidelines for the Care and Use of Laboratory Animals. Genotyping was performed by PCR using tail genomic DNA. To determine the presence of the *Rosa26-CreER^{T2}* allele, genomic DNA was amplified using the following oligonucleotides to generate a wild-type product corresponding to 650 bp and a mutant product corresponding to 825 bp: R26R-univF (5′-AAAGTCGCTCTGAGTTGTTAT-3′), R26R-wtR (5′-GGAGCGGGAGAAATGGATATG-3′), CreER-R1 (5′-CCTGATCCTGGCAATTTCG-3′). To determine the presence of the Runx2 gene's *Floxed* allele, genomic DNA was amplified using the following oligonucleotides to generate a wild-type product corresponding to 320 bp and a mutant band corresponding to 521 bp: (5′-TAAATCCAGATGCCCCTGAG-3′), (5′- TTGAAACCATCCACAGGTGA-3′). To activate the Cre recombinase, mice were intraperitoneally treated with tamoxifen (Sigma) at 70 mg/kg/day for 5 consecutive days.

2.2. Western blotting

Proteins were extracted with lysis buffer (0.1 M Tris [pH 6.7], 4% SDS) and quantified with bicinchoninic acid (BCA) protein assay kit (Takara). Lysate samples (10 μg) were separated on 12.5% SDS-PAGE, and the proteins were subsequently transferred onto 0.45 mm polyvinylidene difluoride (PVDF) membranes (Millipore). Membranes were blocked in PBS supplemented with 5% (w/v) BSA and 0.02% (v/v) Tween 20 for 1 hour at room temperature. The membranes were incubated overnight with primary antibodies at 4 °C. The secondary antibodies were HRP-conjugated (Cell signaling technology). The signals were enhanced with Immobilon ECL Ultra Western HRP Substrate (Merck) and detected by Amersham Imager 600 (GE Healthcare). The following primary antibodies were used: *anti*-Runx2 (1:2000, Cell signaling technology, 12556) and *anti*-β-actin (1:2000, Santa Cruz, sc-47778).

2.3. μCT analyses

The tibiae were analyzed by micro-computer tomography (micro-CT, SkyScan 1174) for 3D image reconstruction as described [19]. Analyses of the trabecular bone volume/tissue volume (BV/TV) and cortical width (Ct.Wi) were calculated based on volumes with a height of 0.3 mm from the growth plate.

2.4. Histology

For paraffin sections, tibiae were fixed with 4% paraformaldehyde (PFA) for 3 days and then decalcified for 7 days using Morse Solution (Wako Pure Chemical Industries Ltd.). The decalcified samples were embedded in paraffin according to the conventional method. Sections (5 μm thickness) were prepared, deparaffinized, and stained with HE. For frozen sections, tibiae were fixed with 4% PFA for 3 days, followed by immersion in 20% sucrose, and then embedded in a super cryoembedding medium (SECTION-LAB Co. Ltd.) and frozen in cooled hexane. Cryosections (10 μm thickness, Leica CM 3050) were generated by Kawamoto's film method (Cryofilm type 2C9) with a tungsten carbide blade. ALP staining was performed using NBT/BCIP Stock Solution (Roche). Tartrate-resistant acid phosphatase (TRAP) staining was performed using Fast Red Violet LB Salt (Sigma). Bone formation rate/bone surface (BFR/BS), which is the calculated rate at which cancellous bone surface and bone volume are replaced annually, was analyzed by the calcein double-labeling method. Calcein (Sigma) was injected into mice twice at 3-day intervals, and mice were sacrificed 2 days after the last injection as described previously [20]. Bone histomorphometric analyses were performed using the OsteoMeasure analysis system (OsteoMetrics) according to standard protocols [21]. For immunofluorescent staining, frozen sections were stained with specific antibodies (Supplemental Table 1). Images were acquired using BX-X710 (Keyence).

2.5. RNA isolation and quantitative RT-PCR (qPCR)

Total RNA was extracted from BM-flushed bone, followed by the synthesis of cDNA using reverse transcriptase and oligo-dT primer. The cDNA samples were then used as templates for real-time PCR analysis, which was performed on AriaMx (Agilent Technologies) using specific primers for each gene (Supplemental Table 2). Expression levels of the genes examined were normalized using Actb expression as an internal control for each sample.

2.6. Statistical analyses

All results are expressed as the mean ± S.E., and statistical significance was determined using the two-tailed and unpaired Student's *t*-tests or two-way analysis of variance with the Tukey–Kramer post-hoc test.

3. Results

3.1. Postnatal Runx2 deletion causes low-turnover osteoporosis and increased bone marrow adiposity

Transgenic mice with a global Runx2 deletion model exhibited skeletal dysplasia and died around birth [10,11]. To investigate postnatal Runx2's role *in vivo*, we generated the *Rosa26-CreER^{T2}; Runx2$^{flox/flox}$* conditional knockout mice, which enabled us to delete the Runx2 gene upon tamoxifen administration. We injected either vehicle (corn oil) or tamoxifen at 70 mg/kg/day for 5 consecutive days in postnatal 4-week-old *Rosa26-CreER^{T2}; Runx2$^{wt/wt}$* or *Rosa26-CreER^{T2}; Runx2$^{flox/flox}$* mice. This was followed by determining Runx2 protein expression in femurs 6 weeks after tamoxifen administration. Western blotting analysis revealed a drastic decrease of Runx2 protein expression in BM and BM-depleted bone tissues only in *Rosa26-CreER^{T2}; Runx2$^{flox/flox}$* mice injected with tamoxifen compared to the other three groups (controls) (Fig. 1A),

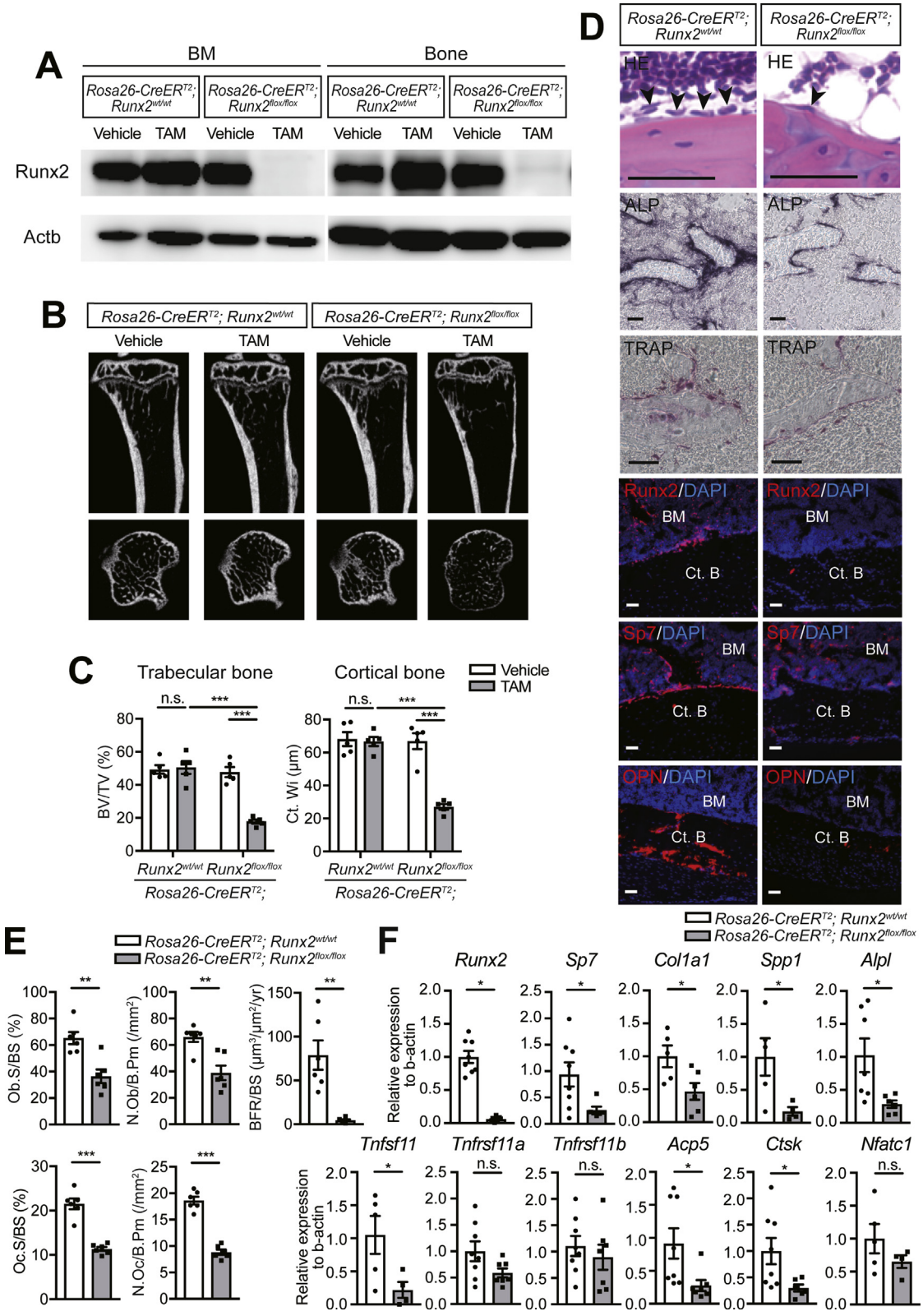

Fig. 1. Postnatal Runx2 deficiency leads to low bone mass. (A) Runx2 protein expression in bone marrow (BM) and BM-depleted bone tissues from *Rosa26-CreER^{T2}; Runx2$^{wt/wt}$* or *Rosa26-CreER^{T2}; Runx2$^{flox/flox}$* mice treated with vehicle or tamoxifen. (B) μCT 2D images of tibiae in *Rosa26-CreER^{T2}; Runx2$^{wt/wt}$* or *Rosa26-CreER^{T2}; Runx2$^{flox/flox}$* mice treated with vehicle or tamoxifen. (C) Quantification of bone parameters in B (n = 5). BV/TV: bone volume/tissue volume; Ct.Wi: Cortical width. (D) Histological analyses of tibiae in *Rosa26-CreER^{T2}; Runx2$^{wt/wt}$* or *Rosa26-CreER^{T2}; Runx2$^{flox/flox}$* mice treated with tamoxifen. Bar = 50 μm. Immunohistochemical analyses of Runx2, Sp7, and Osteopontin (OPN) in tibiae of *Rosa26-CreER^{T2}; Runx2$^{wt/wt}$* or *Rosa26-CreER^{T2}; Runx2$^{flox/flox}$* mice treated with tamoxifen. BM: bone marrow; Ct.B: Cortical bone. Bar = 50 μm. (E) Histomorphometric analyses of tibiae in *Rosa26-CreER^{T2}; Runx2$^{wt/wt}$* or *Rosa26-CreER^{T2}; Runx2$^{flox/flox}$* mice treated with tamoxifen. Ob.S/BS: osteoblast surface per bone surface; N. Ob/B. *Pm*: number of osteoblast per bone perimeter; Oc.S/BS: osteoclast surface per bone surface; N. Oc/B. *Pm*: number of osteoclasts per bone perimeter; BFR: bone formation rate (n = 6). (F) mRNA expression in BM-depleted bone tissues of tibiae in *Rosa26-CreER^{T2}; Runx2$^{wt/wt}$* or *Rosa26-CreER^{T2}; Runx2$^{flox/flox}$* mice treated with tamoxifen (n = 4–8). Statistical significance was determined using the two-tailed and unpaired Student's t-tests or two-way analysis of variance with the Tukey–Kramer post-hoc test, $^{*}p < 0.05$; $^{**}p < 0.01$; $^{***}p < 0.001$, n.s. = not significant.

indicating that this experimental system allowed the successful assessment of postnatal Runx2's role *in vivo*. We first examined the skeletal phenotypes in *Rosa26-CreER^{T2}; Runx2$^{flox/flox}$* conditional knockout mice. In 11-week-old mice, the ablation of Runx2 markedly reduced both trabecular and cortical bone parameters, as indicated by μCT analysis of the tibia (Fig. 1B and C). Histological analyses of tibial sections by HE staining of *Rosa26-CreER^{T2}; Runx2$^{wt/wt}$ or Rosa26-CreER^{T2}; Runx2$^{flox/flox}$* mice revealed that bone lining cells on the surface were greatly reduced, concomitant with a decrease in ALP-positive and TRAP-positive cells. Further, immunohistochemical analyses revealed a significant decrease of Runx2-positive cells, Sp7-positive cells and Osteopontin (OPN) expression in *Rosa26-CreER^{T2}; Runx2$^{flox/flox}$* mice injected with tamoxifen (Fig. 1D). Histomorphometric analyses of the tibiae of *Rosa26-CreER^{T2}; Runx2$^{flox/flox}$* mice injected with tamoxifen showed a significant decrease in osteoblast surface per bone surface (Ob.S/BS), the number of osteoblasts per bone perimeter (N.Ob/B.*P*m), osteoclast surface per bone surface (Oc.S/BS), the number of osteoclasts per bone perimeter (N.Oc/B.*P*m), and the bone formation rate/bone surface (BFR/BS) (Fig. 1E). The femurs of *Rosa26-CreER^{T2}; Runx2$^{flox/flox}$* mice injected with tamoxifen showed a predominant decrease in bone formation markers, including *Runx2*, *Sp7*, *Col1a1*, *Spp1*, and *Alpl*, and bone resorption markers, including *Tnfsf11* (RANKL), *Acp5*, and *Ctsk*, compared to those in *Rosa26-CreER^{T2}; Runx2$^{wt/wt}$* mice injected with tamoxifen. On the contrary, expression of *Tnfsf11a* (RANK), *Tnfsf11b* (OPG) and *Nfatc1* was comparable (Fig. 1F).

Interestingly, histological analyses of *Rosa26-CreER^{T2}; Runx2$^{flox/flox}$* mice injected with tamoxifen also showed a significant adipocyte accumulation in the tibia BM (Fig. 2A and B). Immunohistochemical analyses with antibodies against perilipin (PLIN), which is specifically expressed on droplet surfaces in adipocytes, revealed that PLIN-positive cells increased in the BM of *Rosa26-CreER^{T2}; Runx2$^{flox/flox}$* mice injected with tamoxifen compared to *Rosa26-CreER^{T2}; Runx2$^{wt/wt}$* mice (Fig. 2C).

Thus, postnatal Runx2 deletion causes low-turnover osteoporosis and increased adipocyte accumulation in the BM.

4. Discussion

The *in vivo* postnatal significance of the Runx2 gene has so far remained unknown since global Runx2 deletion (*Runx2$^{-/-}$*) mice die at birth due to severe bone formation defects. Our current findings, using *ROSA26-CreER^{T2}; Runx2$^{flox/flox}$* mice, clearly showed that postnatal Runx2 disruption leads to low-turnover osteoporosis, accumulation of adipocytes in the BM. Although several previous studies have demonstrated Runx2's essential role in osteoblastogenesis and chondrogenesis during skeletogenesis [9–11,22–25], this study, to the best our knowledge, is the first direct demonstration of Runx2's pivotal role in adult bone tissue homeostasis *in vivo*.

Genetically modified mouse models have been developed and analyzed with Runx2 in bone remodeling for several years. Transgenic mice expressing a dominant negative Runx2 (dnRunx2) under the control of a truncated osteocalcin (OG2) promoter exhibited osteopenia [26]; however, transgenic dnRunx2 expression under the control of a *Col1a1* promoter resulted in an anabolic phenotype with increased trabecular bone in young mice [23]. In addition, we recently showed that the osteoblast-specific deletion of *Runx2* using *Col1a1-Cre* mice (*Col1a1-Cre*; *Runx2$^{flox/flox}$*) resulted in no overt skeletal abnormalities [16]. Although these results are contrasting and also, therefore, complicate a clear understanding of Runx2's function, they strongly imply its *in vivo* importance, which is specific to developmental stages. In this study, we clearly demonstrated that the postnatal global deletion of Runx2 in *ROSA26-CreER^{T2}; Runx2$^{flox/flox}$* mice resulted in a low bone mass phenotype, caused by a concomitant decrease in the number of osteoblasts needed for bone formation. Taken together with the fact that postnatal Runx2 deletion increases BM adiposity, the current study suggests that Runx2 is not required for the functional maintenance of mature osteoblasts, but for the commitment/differentiation of the mesenchymal stem cells to the osteoblastic lineage during bone remodeling processes in the adult bone tissues.

In summary, our study demonstrates that postnatal Runx2

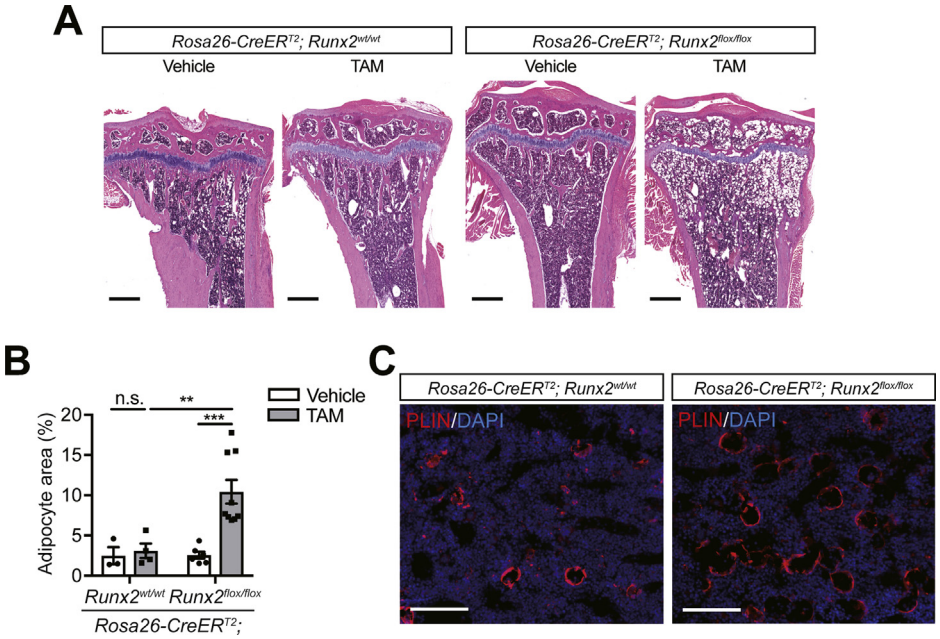

Fig. 2. Postnatal Runx2 deficiency leads to bone marrow (BM) adiposity. (A) HE staining of tibiae in *Rosa26-CreER^{T2}; Runx2$^{wt/wt}$* or *Rosa26-CreER^{T2}; Runx2$^{flox/flox}$* mice treated with vehicle or tamoxifen. Bar = 500 μm. (B) Quantification of adipocyte area per BM area in A (n = 3–9). (C) Immunohistochemical analyses of Perilipin (PLIN) in tibiae of *Rosa26-CreER^{T2}; Runx2$^{wt/wt}$* or *Rosa26-CreER^{T2}; Runx2$^{flox/flox}$* mice treated with tamoxifen. Bar = 100 μm. Statistical significance was determined using the two-way analysis of variance with the Tukey–Kramer post-hoc test, **p < 0.01; ***p < 0.001, n.s. = not significant.

deletion causes aging-associated phenotypes in BM. A further understanding of the mechanism underlying bone and BM aging from the viewpoint of Runx2 function will offer novel feasible therapeutic approaches for aging-related diseases such as osteoporosis.

Conflicts of interest

The authors declare no competing financial interests.

Funding source

This work was supported in part by Grants-in-Aid for Scientific Research to T.T (26460387). from the Ministry of Education, Culture, Sports, Science and Technology, Japan, and in part by research grants to T.T. from the Takeda Science Foundation.

Author contributions

Study design: IT and TT. Study conduct: IT, DY and MY. Data collection: IT, DY, and MY. Data analysis: IT. Data interpretation: IT, EH, MO, TO, TK, TT. Drafting manuscript: IT and TT. IT and TT take responsibility for the integrity of the data analysis.

Acknowledgements

The authors wish to thank the members of the Central Research Laboratory in Okayama University Medical School for technical assistance.

Transparency document

Transparency document related to this article can be found online at https://doi.org/10.1016/j.bbrc.2019.07.014.

Appendix A. Supplementary data

Supplementary data to this article can be found online at https://doi.org/10.1016/j.bbrc.2019.07.014.

References

[1] S.L. Teitelbaum, F.P. Ross, Genetic regulation of osteoclast development and function, Nat. Rev. Genet. 4 (2003) 638–649, https://doi.org/10.1038/nrg1122.
[2] S. Harada, G.A. Rodan, Control of osteoblast function and regulation of bone mass, Nature 423 (2003) 349–355, https://doi.org/10.1038/nature01660.
[3] L.M. Calvi, G.B. Adams, K.W. Weibrecht, J.M. Weber, D.P. Olson, M.C. Knight, R.P. Martin, E. Schipani, P. Divieti, F.R. Bringhurst, L.A. Milner, H.M. Kronenberg, D.T. Scadden, Osteoblastic cells regulate the haematopoietic stem cell niche, Nature 425 (2003) 841–846, https://doi.org/10.1038/nature02040.
[4] J. Zhang, C. Niu, L. Ye, H. Huang, X. He, W.G. Tong, J. Ross, J. Haug, T. Johnson, J.Q. Feng, S. Harris, L.M. Wiedemann, Y. Mishina, L. Li, Identification of the haematopoietic stem cell niche and control of the niche size, Nature 425 (2003) 836–841, https://doi.org/10.1038/nature02041.
[5] O. Naveiras, V. Nardi, P.L. Wenzel, P.V. Hauschka, F. Fahey, G.Q. Daley, Bone-marrow adipocytes as negative regulators of the haematopoietic microenvironment, Nature 460 (2009) 259–263, https://doi.org/10.1038/nature08099.
[6] H. Geiger, G. de Haan, M.C. Florian, The ageing haematopoietic stem cell compartment, Nat. Rev. Immunol. 13 (2013) 376–389, https://doi.org/10.1038/nri3433.
[7] G. Karsenty, The complexities of skeletal biology, Nature 423 (2003) 316–318, https://doi.org/10.1038/nature01654.
[8] B. Lee, K. Thirunavukkarasu, L. Zhou, L. Pastore, A. Baldini, J. Hecht, V. Geoffroy, P. Ducy, G. Karsenty, Missense mutations abolishing DNA binding of the osteoblast-specific transcription factor OSF2/CBFA1 in cleidocranial dysplasia, Nat. Genet. 16 (1997) 307–310, https://doi.org/10.1038/ng0797-307.
[9] S. Mundlos, F. Otto, C. Mundlos, J.B. Mulliken, A.S. Aylsworth, S. Albright, D. Lindhout, W.G. Cole, W. Henn, J.H. Knoll, M.J. Owen, R. Mertelsmann, B.U. Zabel, B.R. Olsen, Mutations involving the transcription factor CBFA1 cause cleidocranial dysplasia, Cell 89 (1997) 773–779.
[10] T. Komori, H. Yagi, S. Nomura, A. Yamaguchi, K. Sasaki, K. Deguchi, Y. Shimizu, R.T. Bronson, Y.H. Gao, M. Inada, M. Sato, R. Okamoto, Y. Kitamura, S. Yoshiki, T. Kishimoto, Targeted disruption of Cbfa1 results in a complete lack of bone formation owing to maturational arrest of osteoblasts, Cell 89 (1997) 755–764.
[11] F. Otto, A.P. Thornell, T. Crompton, A. Denzel, K.C. Gilmour, I.R. Rosewell, G.W. Stamp, R.S. Beddington, S. Mundlos, B.R. Olsen, P.B. Selby, M.J. Owen, Cbfa1, a candidate gene for cleidocranial dysplasia syndrome, is essential for osteoblast differentiation and bone development, Cell 89 (1997) 765–771.
[12] K. Nishikawa, T. Nakashima, S. Takeda, M. Isogai, M. Hamada, A. Kimura, T. Kodama, A. Yamaguchi, M.J. Owen, S. Takahashi, H. Takayanagi, Maf promotes osteoblast differentiation in mice by mediating the age-related switch in mesenchymal cell differentiation, J. Clin. Investig. 120 (2010) 3455–3465, https://doi.org/10.1172/jci42528.
[13] J.H. Hong, E.S. Hwang, M.T. McManus, A. Amsterdam, Y. Tian, R. Kalmukova, E. Mueller, T. Benjamin, B.M. Spiegelman, P.A. Sharp, N. Hopkins, M.B. Yaffe, TAZ, a transcriptional modulator of mesenchymal stem cell differentiation, Science 309 (2005) 1074–1078, https://doi.org/10.1126/science.1110955.
[14] D.M. Thomas, S.A. Carty, D.M. Piscopo, J.S. Lee, W.F. Wang, W.C. Forrester, P.W. Hinds, The retinoblastoma protein acts as a transcriptional coactivator required for osteogenic differentiation, Mol. Cell 8 (2001) 303–316.
[15] P. Bialek, B. Kern, X. Yang, M. Schrock, D. Sosic, N. Hong, H. Wu, K. Yu, D.M. Ornitz, E.N. Olson, M.J. Justice, G. Karsenty, A twist code determines the onset of osteoblast differentiation, Dev. Cell 6 (2004) 423–435.
[16] T. Takarada, E. Hinoi, R. Nakazato, H. Ochi, C. Xu, A. Tsuchikane, S. Takeda, G. Karsenty, T. Abe, H. Kiyonari, Y. Yoneda, An analysis of skeletal development in osteoblast-specific and chondrocyte-specific runt-related transcription factor-2 (Runx2) knockout mice, J. Bone Miner. Res. 28 (2013) 2064–2069, https://doi.org/10.1002/jbmr.1945.
[17] T. Takarada, R. Nakazato, A. Tsuchikane, K. Fujikawa, T. Iezaki, Y. Yoneda, E. Hinoi, Genetic analysis of Runx2 function during intramembranous ossification, Development 143 (2016) 211–218, https://doi.org/10.1242/dev.128793.
[18] A. Ventura, D.G. Kirsch, M.E. McLaughlin, D.A. Tuveson, J. Grimm, L. Lintault, J. Newman, E.E. Reczek, R. Weissleder, T. Jacks, Restoration of p53 function leads to tumour regression in vivo, Nature 445 (2007) 661–665, https://doi.org/10.1038/nature05541.
[19] H.T. Nguyen, M. Ono, Y. Oida, E.S. Hara, T. Komori, K. Akiyama, H.T.T. Nguyen, K.T. Aung, H.T. Pham, I. Tosa, T. Takarada, K. Matsuo, T. Mizoguchi, T. Oohashi, T. Kuboki, Bone marrow cells inhibit BMP-2-induced osteoblast activity in the marrow environment, J. Bone Miner. Res. 34 (2019) 327–332, https://doi.org/10.1002/jbmr.3598.
[20] T. Takarada, C. Xu, H. Ochi, R. Nakazato, D. Yamada, S. Nakamura, A. Kodama, S. Shimba, M. Mieda, K. Fukasawa, K. Ozaki, T. Iezaki, K. Fujikawa, Y. Yoneda, R. Numano, A. Hida, H. Tei, S. Takeda, E. Hinoi, Bone resorption is regulated by circadian clock in osteoblasts, J. Bone Miner. Res. 32 (2017) 872–881, https://doi.org/10.1002/jbmr.3053.
[21] D.W. Dempster, J.E. Compston, M.K. Drezner, F.H. Glorieux, J.A. Kanis, H. Malluche, P.J. Meunier, S.M. Ott, R.R. Recker, A.M. Parfitt, Standardized nomenclature, symbols, and units for bone histomorphometry: a 2012 update of the report of the ASBMR Histomorphometry Nomenclature Committee, J. Bone Miner. Res. 28 (2013) 2–17, https://doi.org/10.1002/jbmr.1805.
[22] P. Ducy, R. Zhang, V. Geoffroy, A.L. Ridall, G. Karsenty, Osf2/Cbfa1: a transcriptional activator of osteoblast differentiation, Cell 89 (1997) 747–754.
[23] Z. Maruyama, C.A. Yoshida, T. Furuichi, N. Amizuka, M. Ito, R. Fukuyama, T. Miyazaki, H. Kitaura, K. Nakamura, T. Fujita, N. Kanatani, T. Moriishi, K. Yamana, W. Liu, H. Kawaguchi, K. Nakamura, T. Komori, Runx2 determines bone maturity and turnover rate in postnatal bone development and is involved in bone loss in estrogen deficiency, Dev. Dynam. 236 (2007) 1876–1890, https://doi.org/10.1002/dvdy.21187.
[24] W. Liu, S. Toyosawa, T. Furuichi, N. Kanatani, C. Yoshida, Y. Liu, M. Himeno, S. Narai, A. Yamaguchi, T. Komori, Overexpression of Cbfa1 in osteoblasts inhibits osteoblast maturation and causes osteopenia with multiple fractures, J. Cell Biol. 155 (2001) 157–166, https://doi.org/10.1083/jcb.200105052.
[25] C. Ueta, M. Iwamoto, N. Kanatani, C. Yoshida, Y. Liu, M. Enomoto-Iwamoto, T. Ohmori, H. Enomoto, K. Nakata, K. Takada, K. Kurisu, T. Komori, Skeletal malformations caused by overexpression of Cbfa1 or its dominant negative form in chondrocytes, J. Cell Biol. 153 (2001) 87–100.
[26] P. Ducy, M. Starbuck, M. Priemel, J. Shen, G. Pinero, V. Geoffroy, M. Amling, G. Karsenty, A Cbfa1-dependent genetic pathway controls bone formation beyond embryonic development, Genes Dev. 13 (1999) 1025–1036.